https://doi.org/10.7494/geom.2026.20.2.67

From Farmland to Cityscape: Urban Growth Simulation in Surkhet Valley, Nepal Using Remote Sensing and CA-Markov Modeling

Padam Bahadur Budha[1] *, Ashutosh Bhardwaj[2], Rajesh Bahadur Thapa[3]

[1] Centre for Space Science and Technology Education in Asia and the Pacific (CSSTEAP), Dehradun, India
[2] Indian Institute of Remote Sensing, Photogrammetry and Remote Sensing Department, Dehradun, India
[3] International Center for Integrated Mountain Development (ICIMOD), Lalitpur, Nepal
* Corresponding author

Abstract: Urbanization is rapidly transforming the spatial and socioeconomic landscape of many emerging cities in Nepal, yet relatively little research has explored these dynamics outside the Kathmandu Valley. This study applies a cellular automata-Markov (CA-Markov) model to simulate and predict land use and land cover (LULC) changes in Surkhet Valley, the core of Birendranagar Municipality, one of Nepal's fastest-growing urban centers. Using Landsat imagery from 1999, 2009, and 2019, alongside spatial and socioeconomic factors, the model captures historical LULC transitions and projects future changes for the years 2029, 2039, and 2049. Model validation was conducted against the 2019 classified LULC map, yielding an overall agreement of 80.65% and a standard kappa statistic of 70.31%, confirming the model's predictive reliability. Results indicate a clear trajectory of urban expansion at the expense of agricultural land. Built-up surfaces is projected to more than double – from 12.43 km² in 2019 to 31.38 km² in 2049, while cultivated land is expected to decline by over 20 km² in the same period. Spatial analysis shows urban growth intensifying around existing centers, highways, and transitional ecotones between forest and cultivation zones. Compared to similar studies in Kathmandu and Biratnagar, Surkhet exhibits a higher normalized rate of urban expansion, highlighting its emerging role in regional development. This research underscores the value of remote sensing and spatial modeling in urban planning and land management. The findings provide essential insights for policymakers to guide sustainable development in Surkhet and other rapidly urbanizing areas across Nepal.

Keywords: GIS-based spatial analysis, Karnali Province, land cover prediction, multi-criteria evaluation (MCE), urban planning

Received: July 13, 2025; accepted: January 27, 2026

E-mails & ORCID iDs: padambudha88@gmail.com, https://orcid.org/0000-0003-1275-3854 (P.B.B); https://orcid.org/0000-0002-9241-5427 (A.B.); https://orcid.org/0000-0003-4467-0148 (R.B.T.).

1. Introduction

Urbanization refers to the concentration of population in specific places, typically cities [1]. It involves people moving into urban areas, which increases population density and expands urban settlements within a specific region [2]. This process intensifies as towns and cities grow in size and capacity. A major driver of urbanization is rural-to-urban migration, where individuals relocate in search of better opportunities, thereby contributing to the rising urban population and the ongoing urbanization process. At its core, urbanization further reflects a shift in the economic base of a society. As urban areas develop, resources and labor transition from the agricultural sector to more urban-based industries [3]. This shift results in a decreasing proportion of the population engaged in farming, while more people pursue employment in services and industrial production. Consequently, traditional agricultural societies gradually transform into modern urban civilizations, characterized by advanced industries, service-oriented economies, high-tech infrastructure, and public service facilities [2].

There are five key drivers of urbanization: industrialization, modernization, globalization, marketization, and administrative/institutional power [2], among which industrialization and modernization particularly involve physical changes to the earth's surface, such as alterations in land cover, which can be effectively monitored through space-based satellite technologies. These technologies allow researchers to assess urban growth in relation to other critical variables, such as population increase, vegetation cover, and shifts in agricultural activity. Moreover, Earth observation tools provide valuable insights into a range of urban indicators, including air pollution and public health, energy efficiency, transportation and mobility, thermal comfort, green spaces, territorial development, vulnerability to environmental hazards, water ecosystems, groundwater status, and urban climate patterns [4].

Closely related to urbanization is urban growth, which refers specifically to the spatial expansion of urbanized land through urban extension. This differs from urban sprawl, which is typically unplanned and occurs in a more dispersed and spontaneous manner [5]. Urban growth can result from city-specific developments or broader economic changes that either enhance agglomeration forces, such as shared infrastructure and labor markets, or reduce congestion and other limiting factors [6]. Urban growth is commonly understood through three interrelated dimensions: changes in population size, improvements in economic performance, and the physical expansion of built-up areas [7]. In addition to population increase, urban growth encompasses a range of dynamic processes, including technological innovation, shifts in industrial composition, the expansion of commuting and transport infrastructure, and the evolution of integrated urban systems [6]. Given that most economic activities are concentrated in cities, the growth and proliferation of urban centers are closely tied to the strengthening of national economies.

Remote sensing has become a key tool in assessing and monitoring urban growth and its spatial patterns. Both optical and microwave remote sensing technologies offer

valuable data for observing changes in the urban environment over time. The long-term availability and continuity of satellite imagery, particularly from the Landsat program, have enabled detailed, multi-decadal analyses of urban expansion. For example, [8] emphasized the role of Landsat data in supporting consistent monitoring of urban dynamics, while [9] used Landsat imagery dating back to 1980 to study four decades of urbanization across six major cities in China's Yangtze River Delta. The combination of fine spatial resolution and frequent revisit cycles provided by modern satellites makes it possible to capture even subtle changes in land cover caused by urban development.

Earth observation systems have been especially useful in mapping urban growth and predicting land use and land cover (LULC) changes. These systems enable the monitoring of various urban indicators, including spatial expansion, population density, and environmental parameters such as air and water quality [4]. By analyzing both historical and current LULC data, researchers can identify trends and estimate future land use patterns. This capability is particularly valuable for integrating with urban planning initiatives and developing sustainable growth strategies.

Urban growth models utilize geospatial datasets to simulate and project future urban expansion with a high degree of precision. [10] reviewed six major types of geospatially based urban growth models, including cellular automata (CA) [11–15], artificial neural networks (ANN) [16–18], fractal models [19, 20], linear/logistic regression models [21, 22], agent-based models [23, 24], and decision tree (DT) models [25]. These models rely on present and past LULC data, along with various socio-economic and environmental variables, to simulate complex urban growth processes and support evidence-based decision-making.

In Nepal, only a few studies have been conducted focusing on the Kathmandu Valley [26, 27], which consists of the capital city of Nepal and other major cities. These studies highlighted significant LULC changes over past decades, showing that urban built-up areas have expanded largely at the expense of green vegetation and cultivated land. Such information on spatial urban expansion is critical for urban simulations that aim to predict, plan, and manage future LULC dynamics. Meanwhile, most studies have focused on Kathmandu and its surrounding areas [18, 28–30], yet rapidly expanding cities across Nepal remain understudied, and similar spatial modeling is required for them to support planners in timely decision-making. This research explores one of the cities in western Nepal that is experiencing rapid urban growth.

The focus of this study is Surkhet Valley, the core of Birendranagar Municipality – the capital of Karnali Province. This makes it an administrative center and key socio-economic hub in western Nepal. Surkhet Valley also represents one of the rapidly transforming urban landscapes in Nepal, yet it remains unexplored in terms of scientific urban growth modeling. Recent reports from the Ministry of Urban Development (MoUD) indicate that this area has experienced a significant surge in population, making Birendranagar one of the fastest-growing cities in Nepal [31]. This population increase over the past decade was primarily driven by rural-to-urban migration, expansion of service sectors, and improved regional connectivity.

This growth has begun to exert considerable pressure on agricultural land, water resources, and ecological systems within Surkhet Valley. Moreover, the valley is surrounded by Siwalik and Mahabharat ranges that limit horizontal urban expansion and unplanned growth can pose risk to the limited productive land. Thus, understanding the patterns and future transformations of the LULC in the area becomes vital. Consequently, conducting urban growth modeling in Surkhet Valley is both timely and essential for sustainably managing the valley's ongoing spatial transformation. Future land-use predictions and their spatial distribution can provide planners and decision-makers with strategic insights for preparing land-use plans and development strategies. This study also has broader implications for managing urbanization in other rapidly growing mid-hill cities of Nepal.

2. Materials and Methods

2.1. Study Area

The research area, as depicted in Figure 1, encompasses Surkhet Valley, which forms the core of Birendranagar Municipality.

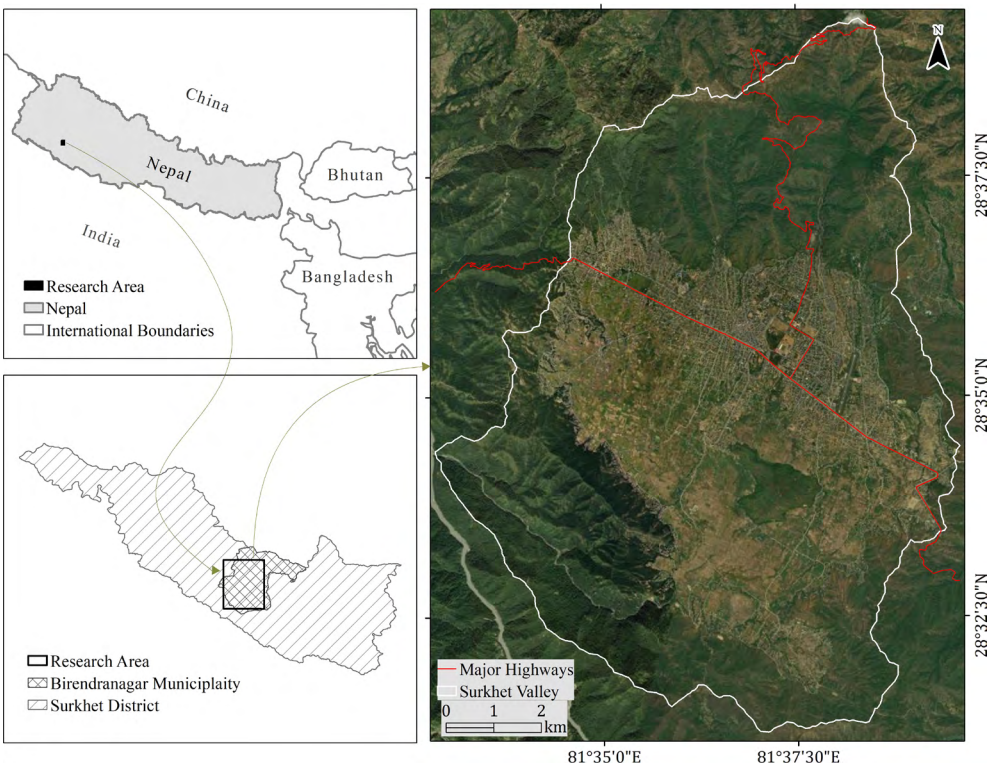

Fig. 1. Geographic location of the research area in Nepal with Surkhet Valley depicted on satellite imagery

This valley accounts for approximately 42% of the municipality's total area, with most of the built-up zone concentrated in its central region. Covering 103.15 km², the valley is surrounded by hills on all sides and features a drainage outlet in the south, where water flows into the Bheri River before eventually joining the Karnali River.

Located in Nepal's Siwalik region, the city lies at a lower elevation (from 340 m to 1980 m) as compared to much of the country. Its climate ranges from tropical to subtropical, and the combination of favorable topography and climate makes the valley particularly well-suited for human settlement.

As the capital of Karnali Province, the city enjoys better infrastructure and services than many other regions, positioning it as a key center for business, education, and other sectors. Since its designation as the provincial capital, numerous infrastructure development projects have been launched, and existing roads have been expanded. These improvements, coupled with population growth, have driven the continued spatial expansion of the city's built-up area.

2.2. Data Sources and Preparation

The primary datasets for this analysis were LULC maps for the years 1999, 2009, and 2019 [32]. Constraint layers for water bodies and built-up areas were extracted from the LULC map of 2009, in which no further growth was assumed to take place. Additional spatial datasets included a digital elevation model (DEM) obtained from the Alaska Satellite Facility. This DEM was a radiometrically terrain-corrected product derived from ALOS PALSAR data, with a spatial resolution of 12.5 m. Vector data for roads, small water bodies, and urban centers were extracted from high-resolution Google Earth imagery to support the modeling of socioeconomic factors.

All LULC maps were prepared using level 1 terrain precision (L1TP) products of Landsat satellite with path and row of 144/40 and 143/40. Images of date November 9, 1999 (Landsat 7), November 5, 2009 (Landsat 5), and November 17, 2019 (Landsat 8) were exercised in this research. As the Landsat 7 image was used only for the year 1999, there was no issue of the scan line corrector (SLC) error. Each map was classified into six major classes: built-up area, cultivation, forest, sand, shrub/grassland, and water. The maps were spatially aligned, using the same pixel resolution and coordinate reference system, to ensure consistency for overlay analysis and modeling.

2.3. Method

The LULC change simulation was performed using the CA-Markov model available in the IDRISI software suite. This model combines the temporal dynamics of a Markov chain with the spatial dynamics of cellular automata to simulate future land-use changes. The workflow for the modeling process is summarized in Figure 2.

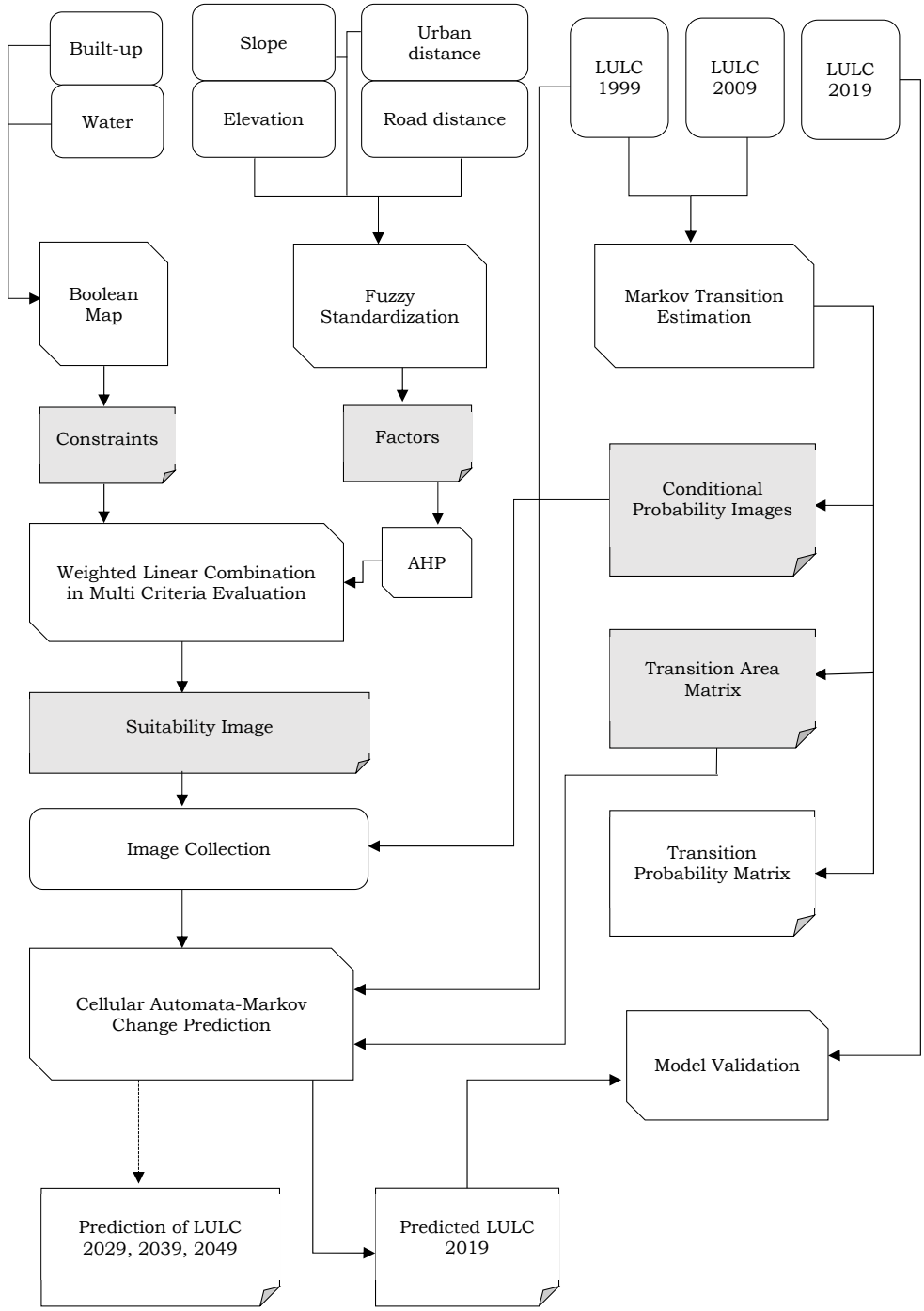

Fig. 2. Process of future LULC prediction using CA-Markov model

Constraints and Factor Maps

Two types of inputs were used to influence the model:

1) constraints (built-up and water bodies);
2) factors (elevation, road distance, slope, and urban distance).

These are illustrated in Figure 3.

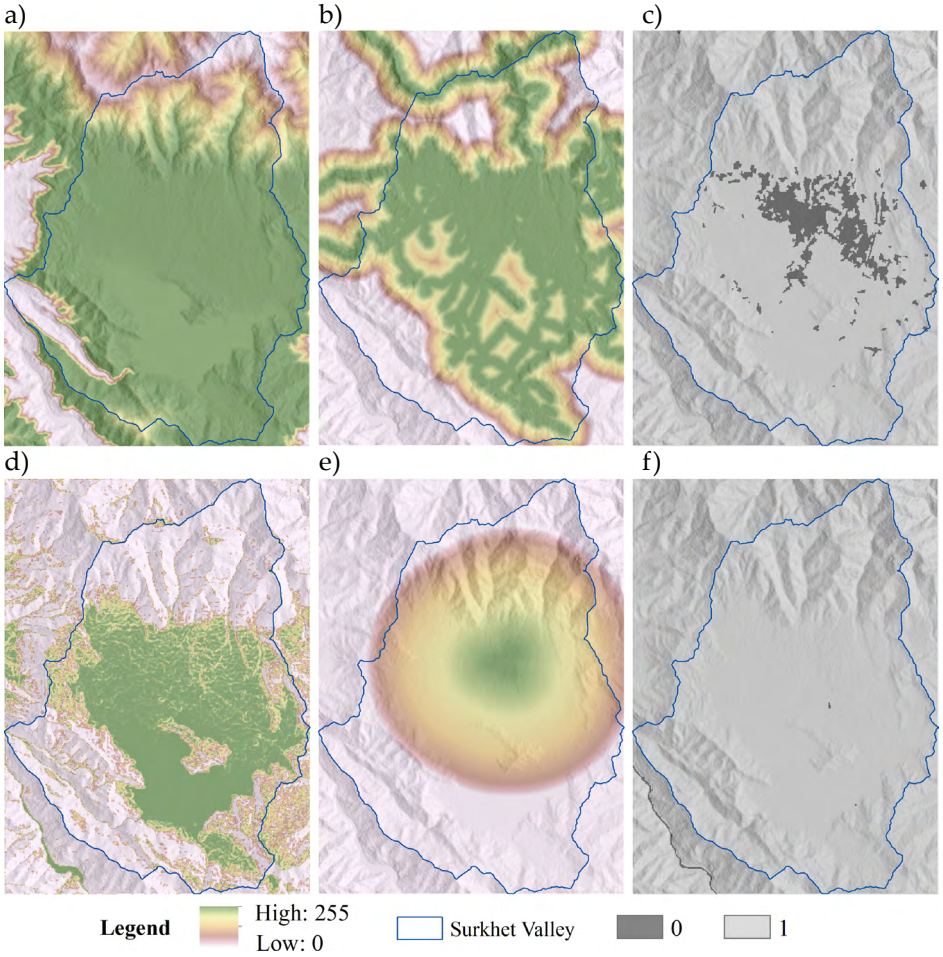

Fig. 3. Constraints (c and f) and factors (a, b, d, and e) used in the CA-Markov model: a) elevation; b) road distance; c) built-up; d) slope; e) urban distance; f) water bodies

Constraints define areas where land cover change is not allowed. These included existing built-up areas and water bodies, extracted from the 2009 LULC map. The constraint map was converted into a Boolean raster, where a value of 0 represented areas restricted from change and a value of 1 indicated areas where change could occur.

Factors are continuous variables that influence the likelihood of land cover transition. Among the four factor layers used in this study, two were topographic factors (elevation and slope derived from the DEM) and two were socioeconomic factors (distance from roads and distance from urban centers).

Each factor layer was standardized using fuzzy logic in IDRISI, with values ranging from 0 to 255, where higher values indicated greater suitability for change. The fuzzy membership functions and control points used for standardization are presented in Table 1. These were derived from the literature review and from the topographic characteristics of the study area.

The use of both constraint and factor layers allows the model to realistically simulate spatial patterns of land use change. While constraint layers strictly limit transitions in areas where change is not possible, factor layers guide the spatial allocation of future land use by representing the influence of environmental and accessibility conditions. In this study, the combined effect of topographic and socioeconomic factors helps capture the development tendency toward areas with favorable terrain and better connectivity. This approach improves the spatial reliability of the transition suitability maps generated for the CA-Markov model.

Table 1. Fuzzy standardization parameters for suitability factors

Factor	Fuzzy Membership Function	Fuzzy Membership Shape	Control Points
Elevation	sigmoidal	symmetric	500 m, 600 m, 700 m, 1,600 m
Road distance	linear	monotonically decreasing	100 m, 1,000 m
Slope	sigmoidal	monotonically decreasing	0°, 15°
Urban distance	linear	monotonically decreasing	60 m, 4,500 m

The standardized factors and constraints were combined into a single suitability map using a weighted linear combination (WLC) approach within the multi-criteria evaluation (MCE) module in IDRISI. The analytic hierarchy process (AHP) was used to estimate the weights, with the ranking informed by the literature. This process produced weights of 0.0959 for elevation, 0.4430 for road distance, 0.1828 for slope, and 0.2783 for urban distance. The consistency ratio for this AHP analysis was 0.014 reflecting consistent judgments in pairwise comparisons.

The final output from the MCE process was a suitability map (8-bit raster), where pixel values ranged from 0 (least suitable for land-cover change) to 255 (most suitable). This map is shown in Figure 4, where areas with the highest suitability were visually represented in white, pink and blue colors, while areas excluded from change (water and built-up zones) appeared dark brown.

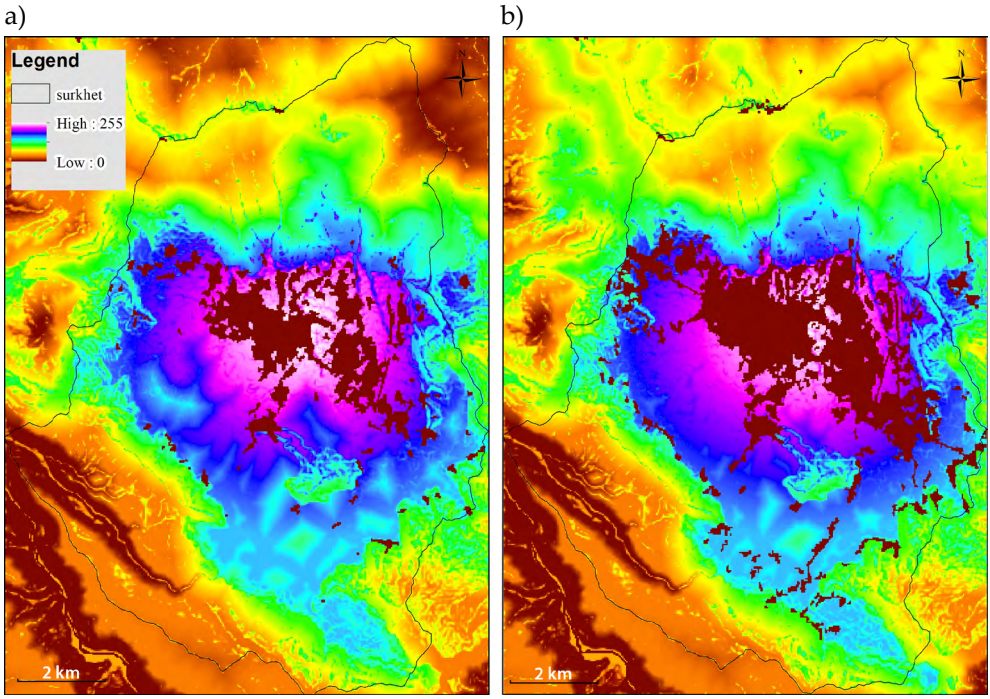

Fig. 4. Suitability map produced by combining all the factors and constraints for 2009 (a) and 2019 (b)

Markov Chain Analysis

The Markov chain component of the model estimates the probability of transition between LULC classes over time. This analysis used classified LULC maps from 1999 and 2009 to estimate the probability matrix and conditional probability maps to be used in the prediction of LULC for 2019. The transition period between images was 10 years, and the prediction was also made for a 10-year forward period (i.e., 2009 to 2019). The built-up constraint was updated while making suitability maps for subsequent years.

The transition matrix summarizes the likelihood that a given LULC class will either remain unchanged or transition into another class over the next decade. Table 2 presents the transition probabilities derived from the 1999 and 2009 LULC maps. Similarly, Figure 5 depicts the probability images, which constitute a key input to the model.

The matrix indicates that, for example, built-up areas had an 80.86% chance of remaining same and a 12.42% chance of being converted to cultivated land. Similarly, forests had an 87.91% probability of persistence and a 6.42% chance of converting to shrub/grassland. These probabilities formed the basis for simulating future LULC scenarios. The areas that changed into built-up were primarily from cultivation, sand, and shrub-grassland as indicated by the given probabilities.

Table 2. Transition matrix probability derived from LULC images of 1999 and 2009. Rows represent LULC classes in 1999 (initial state), columns represent LULC classes in 2009 (subsequent state), values indicate transition probabilities

LULC Class	Built-up	Cultivation	Forest	Sand	Shrub/Grassland	Water
Built-up	0.8086	0.1242	0.0252	0	0.0420	0
Cultivation	0.0878	0.8141	0.0556	0.0010	0.0411	0.0003
Forest	0.0067	0.0480	0.8791	0.0018	0.0642	0.0003
Sand	0.2836	0.2690	0.0719	0.3368	0.0167	0.0219
Shrub/grassland	0.0734	0.2646	0.2919	0.0066	0.3631	0.0003
Water	0	0.0263	0.1093	0.0891	0.0243	0.7510

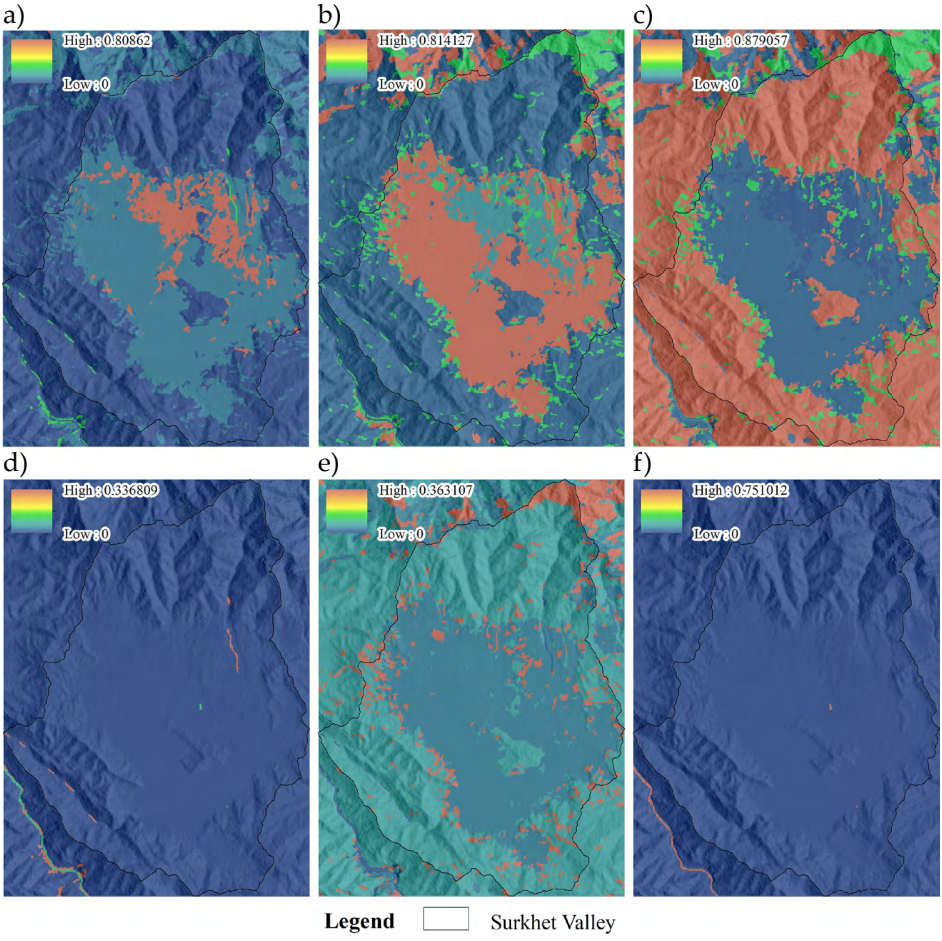

Fig. 5. Conditional probability images derived from 1999 and 2009 LULC maps: a) built-up; b) cultivation; c) forest; d) sand; e) shrub/grassland; f) water

Cellular Automata Simulation

The cellular automata component allocates land use transitions spatially by considering both transition probabilities and neighborhood influence. This approach enables the model to reproduce realistic patterns of land development and expansion. As a result, the simulated map reflects both the statistical transition trends and the spatial structure of land use change.

The CA-Markov model used three main inputs:

1) base year LULC map: the 2009 map was used to simulate 2019;
2) transition area matrix: derived from Markov analysis;
3) suitability and probability images: created through the MCE and Markov modules.

The spatial dynamics were modeled using a standard 5 × 5 contiguity filter with 10 iterations. This allowed the simulation to account for spatial dependencies and neighborhood effects. The final output was the simulated LULC map for 2019.

Model Validation and Future Prediction

The accuracy of the CA-Markov model was validated by comparing the simulated 2019 LULC map with the actual classified map for the same year. IDRISI's validation tools were used to compute statistical measures, including kappa statistics. A high kappa value indicated a strong agreement between the predicted and observed LULC distributions, confirming the model's reliability.

Upon successful validation, the model was applied to predict LULC for the future years 2029, 2039, and 2049. Each prediction used sequential 10-year LULC image pairs:

– 2009–2019 for predicting 2029;
– 2019–2029 for predicting 2039;
– 2029–2039 for predicting 2049.

For each time step, the most recent classified or simulated LULC map served as the base year. Suitability maps were updated using the latest available information. Static factors such as slope and elevation remained unchanged, constraints were extracted from the base-year LULC map, and socioeconomic factors were updated using recent Google Earth imagery.

3. Results

3.1. LULC Prediction Modeling

Measurements of urban growth and simulations of future LULC are essential components of urban studies, as they support policymakers and urban planners. It is evident that urban growth is occurring in Surkhet Valley [33], and the built-up area is increasing at a very high rate. Birendranagar Municipality is one of seven cities in Nepal – and the only one in western Nepal – with urban growth rates exceeding 5% [31].

The predicted LULC map for 2019 displayed smoother boundaries between LULC classes, as smaller patches had coalesced and, in some cases, vanished into larger categories. Figure 6 shows a comparison between the CA-Markov model's predicted LULC map and the classified LULC map based on the 2019 Landsat image. Each LULC class in the predicted map differs slightly from the corresponding class in the classified map. Major differences were noted in the built-up, cultivation, and forest categories. In the predicted map, the built-up area expanded primarily around the existing built-up zones of 2009 and along road networks. In this map, smaller patches merged into the dominant surrounding classes, reducing visual fragmentation.

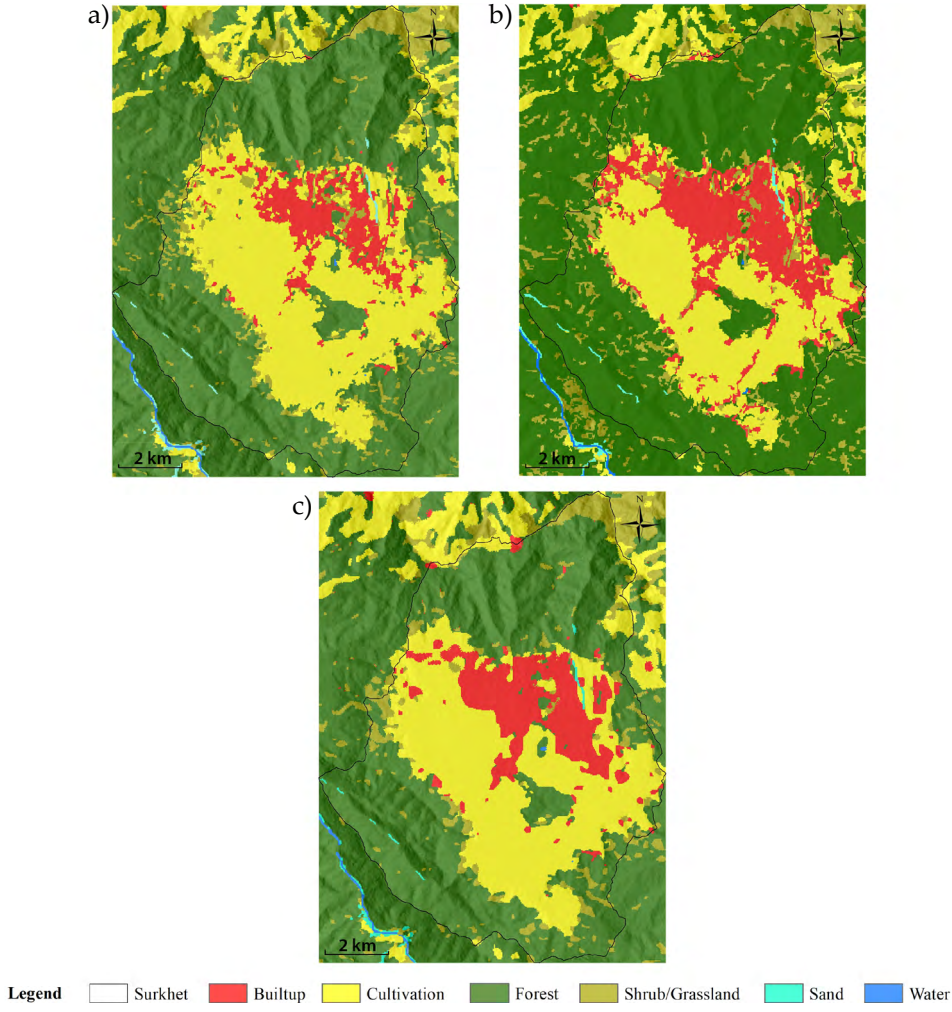

Fig. 6. Classified LULC map of 2009 (a) and 2019 (b) and model predicted LULC map of 2019 (c)

Source: [32] (figures a and b)

The predicted built-up area was 3.36% smaller than that in the classified map. Similarly, forest and shrub/grassland areas were also slightly lower in the predicted LULC. The only LULC class showing a notable increase in the predicted map was cultivation, which was 6.59% higher. The sand and water classes had nearly identical areas in both the predicted and classified maps. Figure 7 presents a comparison of the area covered by each LULC class in the predicted and classified maps.

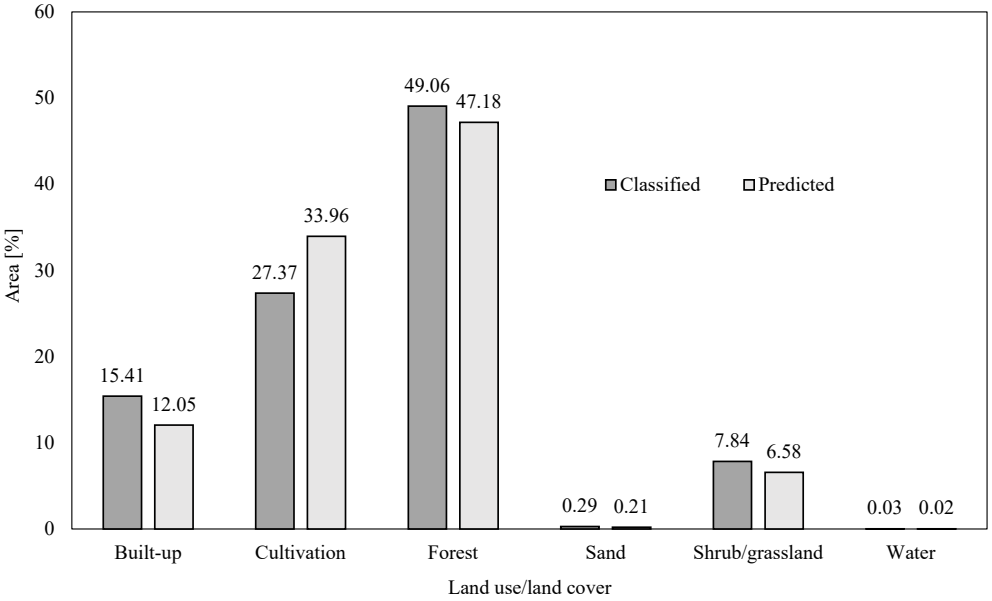

Fig. 7. Comparisons of area (in percentages) for each class of classified and predicted LULC of year 2019

3.2. LULC Prediction Validation

The prediction model's performance was evaluated by comparing the predicted and classified maps which provided various kappa statistics. The overall agreement between the predicted and observed 2019 LULC maps was 80.65%. The kappa indices produced were:

- kappa for no information (K_{no}): 76.77%
- kappa for grid cell-level location ($K_{location}$): 78.23%
- kappa for stratum-level location ($K_{locationStrata}$): 78.23%
- standard kappa ($K_{standard}$): 70.31%

$K_{standard}$, considered the overall kappa, exceeded the commonly accepted threshold of 70%, indicating that the CA-Markov prediction model performed satisfactorily.

3.3. Further Prediction

The predicted spatial coverage of LULC classes for the years 2019, 2029, 2039, and 2049 is presented in Table 3. The driving factors and constraints used in the model were critical in determining urban expansion. While all LULC categories were predicted, the main focus was on the built-up category. The model predicts significant growth in built-up areas, accompanied by a decline in cultivated land. The built-up area is expected to increase from 12.43 km² in 2019 to 31.38 km² by 2049. In contrast, the area under cultivation is projected to decrease from 35.03 km² in 2019 to 14.64 km² in 2049.

Table 3. Area [km²] of LULC classes in CA-Markov predicted maps for years 2019, 2029, 2039, and 2049

Year	LULC class					
	Built-up	Cultivation	Forest	Sand	Shrub/grassland	Water
2019	12.43	35.03	48.66	0.21	6.79	0.03
2029	21.14	23.59	50.39	0.30	7.68	0.06
2039	26.35	19.10	49.22	0.30	8.10	0.09
2049	31.38	14.64	48.20	0.30	8.52	0.11

The predicted 2019 LULC map identified forests, cultivation, and built-up areas as the dominant land cover types. Forests and cultivation occupied 48.66 km² and 35.03 km² respectively – together accounting for approximately 83% of Surkhet Valley's total area. The built-up area measured 12.43 km², which was 3.36% lower than the observed extent for the same year. Built-up expansion was primarily concentrated around existing urban centers and highways. Small built-up patches were also observed on the northern ridge, indicating potential growth zones for fringe towns. Some built-up patches encircled a central forest patch. Meanwhile, shrub/grassland, covering 6.79 km², served as an ecotonal strips between cultivation and forest. Built-up development was also emerging along these strips. Water bodies occupied the smallest area, representing only 0.024% of the valley's 103.15 km².

In the 2029 prediction (Fig. 8), both the built-up and water classes increased. In this year additional 5.18% of Surkhet Valley was projected to convert into built-up class, totaling 21.14 km². Built-up patches expanded along the boundary between forests and cultivated land, especially in the north–south corridor near major urban zones. Surface with cultivation was projected to shrink to 23.59 km², a decrease of 4.65 km² from area of 2019. It appears that after 2032, the built-up would surpass the cultivation, whereas forest and shrub/grassland coverage reflects little change in that time. The area of sand remained constant at 0.30 km², while water showed a minor increase.

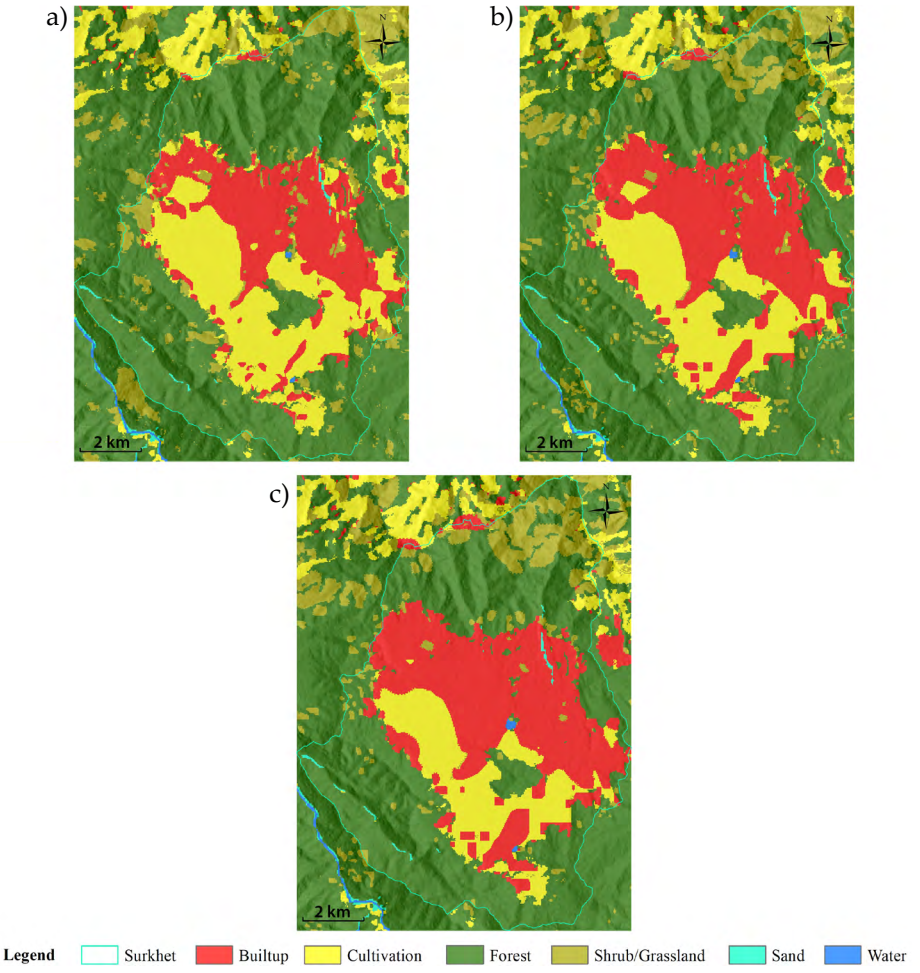

Fig. 8. LULC maps of Surkhet Valley predicted by the model for 2029 (a), 2039 (b), and 2049 (c)

By 2039 (Fig. 8), the built-up was predicted to reach 26.35 km², surpassing cultivation, which would drop further down to 19.10 km². The northern half of the valley floor was expected to be largely urbanized, making up nearly one-third of Surkhet Valley. Only small patches of cultivated land and isolated sand strips would remain. Area of forest was expected to decline slightly to 49.22 km², while shrub/grassland would rise to 8.10 km².

As shown in Figure 8, most of the valley floor in 2019 was covered by cultivation rather than built-up. However, by 2049, this pattern is projected to reverse, with urban areas expanding and replacing agricultural land. Comparing 2049 to 2019, the built-up area would increase by 18.95 km² (an 18.37% rise), reaching 31.38 km² or 30.42% of Surkhet Valley. Meanwhile, cultivation would drop

from 35.03 km² to 14.64 km² – a decrease of 20.39 km². These trends suggest continued urban expansion at the expense of agricultural lands.

The greatest spatial changes are predicted to occur between 2019 and 2029. In the following decades, the rate of change is expected to slow down, but the built-up area is still expected to nearly double over the next 30 years. When the projected areas of future LULC classes are plotted, the model results indicate that built-up areas will exceed cultivated land around 2032.

4. Discussion

When reviewing past studies on urban growth modeling in Nepal, it was found that studies on cities like Kirtipur [28] and Biratnagar [34] had simulations only up to 2020. Therefore, their findings cannot be directly compared with the present research. For comparisons of future LULC change trends, reference can be made to research or urban expansion modeling of 24 cities from Kathmandu Valley and Kabhrepalanchok District (KVKD) [30], although this study was conducted over a much larger area of 1,215.23 km².

Figure 9 presents the rates of LULC change for the KVKD and Surkhet areas.

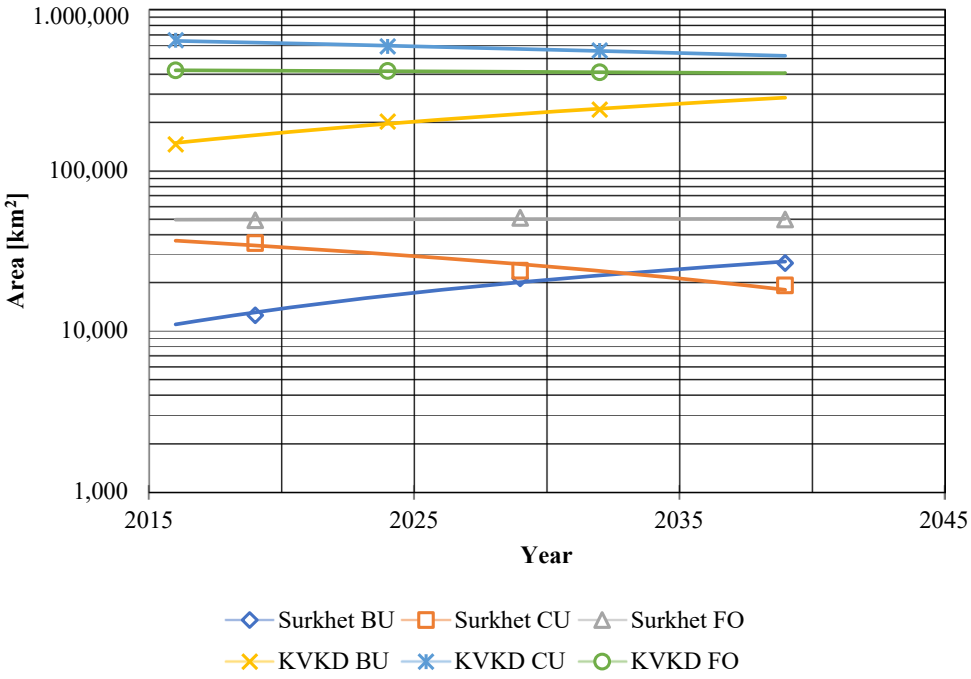

Fig. 9. Future trends in major LULC of Surkhet Valley and KVKD: BU – built-up, CU – cultivation, and FO – forest

Source: data of KVKD from [30]

A similar trend of increasing built-up area and decreasing cultivated land was observed in both of the research locations. From research of KVKD [30], the built-up area, which was 144.35 km² in 2016, is projected to increase to 238.17 km² by 2032. Conversely, cultivated land is expected to decline from 641.96 km² to 555.48 km² over the same period. When comparing these projections with those of the present study, it was found that Surkhet Valley is likely to experience a higher rate of change in both built-up and cultivated land areas. From the trend of Surkhet Valley in Figure 9, it appears that after 2032 the area covered by built-up land will be higher than that of cultivated land.

The study of KVKD [30] covered a broader area, resulting in higher overall change quantities than those observed in Surkhet Valley. However, the study did not specify which cities experienced the most significant changes. Despite this, the trends of increased built-up area and decreased cultivated land were consistent across both studies. When normalized by total area, the rate of change in Surkhet appears more rapid. Thus, although Surkhet Valley is smaller in size, it exhibits a greater rate of change. This trend is expected to continue over the next three decades, potentially doubling the built-up area while reducing cultivated land by half.

The results indicated probabilities of conversions from cultivated lands, shrubs/grasslands, and sand areas into built-up areas, yet the simulation results showed that all LULC classes had increased by the end of 2049, with the exception of cultivated land, which decreased. There can be interchanges of LULC classes between cultivated land and shrubs/grassland and between shrubs/grasslands and forests, besides major shifts of cultivated land into built-up areas.

Looking at the spatial pattern of built-up expansion in Figure 10, the growth was mostly observed around areas with a dense network of roads. However, the built-up expansion was constrained in the northern and southern parts of the valley due to steep slopes and the presence of forested terrain. It can also be noted that areas with less developed road networks, particularly in the central agricultural area, experienced limited built-up growth. These findings suggest that urban expansion is not driven solely by the conversion of fertile agricultural land; rather, the increasing density and connectivity of road infrastructure play a decisive role in accelerating the spread of impervious, concrete-covered surfaces.

The validation module computed model accuracy metrics, showing an agreement of 0.8065. This measure of agreement comprised three components: agreement due to location (grid cell or strata), agreement due to quantity, and agreement due to chance. Conversely, disagreement included components attributable to location and quantity [35]. Accordingly, the agreement due to location, quantity, and chance measured 0.4584, 0.1814, and 0.1667, respectively. The measures of disagreement due to location and quantity were 0.1275 and 0.0660, respectively.

The CA-Markov model has also been applied in other studies, including Kirtipur Municipality [28], the Kathmandu Valley with Kavrepalanchok District [30], and Biratnagar Metropolitan City [34], whose accuracies are summarized in Table 4.

The overall accuracies (K_{no}) for these studies were 0.8815, 0.91, and 0.8501, respectively. For comparison, a study using multilayer perceptron neural network (MLPNN) [18], an ANN-based model, reported an accuracy of 86.26%. Although these studies demonstrated higher accuracy than the present research, they did not explicitly state whether the observed agreement was due to chance, location, or quantity.

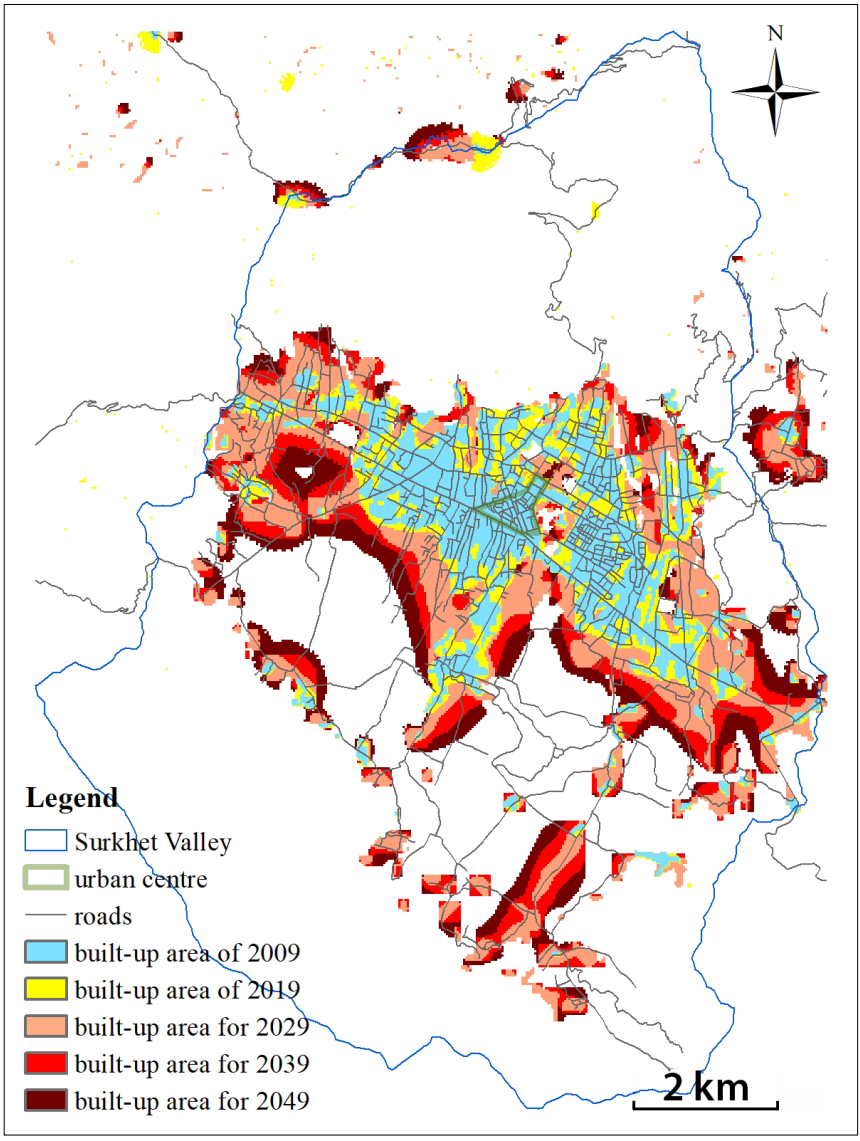

Fig. 10. Built-up surface change (2009–2049)
in Surkhet Valley with road network and urban center overlay

Table 4. Summary of accuracy in urban simulation studies in Nepal

Study Area	Method Used	Accuracy (K_{no})
Kathmandu Valley [18]	MLPNN-Markov	0.8626
Kirtipur Municipality [28]	CA Markov chain	0.8815
Kathmandu Valley and Kavrepalanchok District [30]	CA Markov chain	0.9100
Biratnagar City [34]	CA Markov chain	0.8509
Surkhet Valley (Birendranagar City) (present research)	CA Markov chain	0.7677

Nevertheless, the model in this study also performed well, achieving an agreement of 80.65% and overall accuracy of 76.77% for the simulated 2019 LULC map. The relatively lower accuracy may be attributed to variability in the suitability maps used during model calibration. Accuracy can improve when LULC maps derived from higher resolution image are applied in the simulation or if suitability maps are calibrated better [36].

5. Conclusion

This study successfully modeled and predicted LULC changes in Surkhet Valley using the CA-Markov model, providing valuable insights into urban growth trends and their implications for sustainable urban planning. The results indicate a clear and accelerating trend of urban expansion, particularly around existing urban centers and major road corridors, with built-up areas projected to more than double from 2019 to 2049. Conversely, cultivated land is expected to decline sharply, signaling a shift in land use priorities and pressures on agricultural resources.

The model showed acceptable predictive performance, with an overall agreement of 80.65% between the predicted and observed 2019 maps. Kappa statistics, including a $K_{standard}$ value of 70.31%, confirmed the model's reliability in capturing spatial and categorical changes.

Comparative analysis with LULC change trends in the Kathmandu Valley highlighted that although Surkhet is smaller in size, its rate of urban expansion is higher when normalized by area. The study forecasts that built-up areas will surpass cultivated land around 2032, suggesting a pivotal transition in the valley's land-use dynamics.

Overall, this research highlights the critical role of predictive modeling in guiding proactive urban planning and resource management. The findings serve as a baseline for local authorities and policymakers to monitor land use changes and implement balanced development strategies that protect ecological zones while accommodating urban growth.

Funding

This research received no specific grant from any funding agency in the public, commercial, or not-for-profit sectors.

CRediT Author Contribution

P. B.: conceptualization, formal analysis, investigation, resources, data acquisition, writing – original draft preparation, writing – review and editing, visualization.

A. B.: review and editing, supervision.

R. B. T.: review and editing, supervision.

Declaration of Competing Interests

The authors declare that they have no known competing financial interests or personal relationships that could have appeared to influence the work reported in this paper.

Data Availability

This study is based on Level-1 Terrain Precision (L1TP) Landsat satellite imagery provided by the United States Geological Survey (USGS). The datasets were downloaded from the USGS EarthExplorer platform and are publicly available at no cost. The corresponding path/row and dates of acquisition are provided in the main text of the manuscript.

Use of Generative AI and AI-Assisted Technologies

No generative AI or AI-assisted technologies were employed in the preparation of this manuscript.

References

[1] Tisdale H.: *The process of urbanization*. Social Forces, vol. 20(3), 1942, pp. 311–316. https://doi.org/10.1093/sf/20.3.311.

[2] Gu C.: *Urbanization: Processes and driving forces.* Science China Earth Sciences, vol. 62(9), 2019, pp. 1351–1360. https://doi.org/10.1007/s11430-018-9359-y.

[3] Henderson J.V.: *Urbanization and growth*, [in:] Aghion P., Durlauf S.N. (eds.), *Handbook of Economic Growth. Volume 1, Part B*, Elsevier, 2005, pp. 1543–1591. https://doi.org/10.1016/S1574-0684(05)01024-5.

[4] Chrysoulakis N., Feigenwinter C., Triantakonstantis D., Penyevskiy I., Tal A., Parlow E., Fleishman G., Düzgün S., Esch T., Marconcini M.: *A conceptual list of indicators for urban planning and management based on earth observation*. ISPRS International Journal of Geo-Information, vol. 3(3), 2014, pp. 980–1002. https://doi.org/10.3390/ijgi3030980.

[5] Viana C.M., Oliveira S., Oliveira S.C., Rocha J.: *Land use/land cover change detection and urban sprawl analysis*, [in:] Pourghasemi H.R., Gokceoglu C. (eds.), *Spatial Modeling in GIS and R for Earth and Environmental Sciences*, Elsevier, 2019, pp. 621–651. https://doi.org/10.1016/b978-0-12-815226-3.00029-6.

[6] Ioannide Y.M., Rossi-Hansberg E.: *Urban growth*, [in:] Durlauf S.N., Blume L.E. (eds.), *Economic Growth*, The New Palgrave Economics Collection, Palgrave Macmillan, London 2010, pp. 264–269. https://doi.org/10.1057/9780230280823_33.

[7] Reis J.P., Silva E.A., Pinho P.: *Spatial metrics to study urban patterns in growing and shrinking cities*. Urban Geography, vol. 37(2), 2015, pp. 246–271. https://doi.org/10.1080/02723638.2015.1096118.

[8] Moeller M.S.: *Remote sensing for the monitoring of urban growth patterns*. ISPRS Archives, vol. XXXVI-8/W27, 2005. https://www.isprs.org/proceedings/xxxvi/8-w27/moeller.pdf [access: November 5, 2020].

[9] Fang C., Zhao S.: *A comparative study of spatiotemporal patterns of urban expansion in six major cities of the Yangtze River Delta from 1980 to 2015*. Ecosystem Health and Sustainability, vol. 4(4), 2018, pp. 95–114. https://doi.org/10.1080/20964129.2018.1469960.

[10] Musa S.I., Hashim M., Reba M.N.M.: *A review of geospatial-based urban growth models and modelling initiatives*. Geocarto International, vol. 32(80), 2017, pp. 813–833. https://doi.org/10.1080/10106049.2016.1213891.

[11] Clarke K.C., Hoppen S., Gaydos L.: *A self-modifying cellular automaton model of historical urbanization in the San Francisco Bay area*. Environment and Planning B: Planning and Design, vol. 24(2), 1997, pp. 247–261. https://doi.org/10.1068/b240247.

[12] Falah N., Karimi A., Harandi A.T.: *Urban growth modeling using cellular automata model and AHP (case study: Qazvin city)*. Modeling Earth Systems and Environment, vol. 6(1), 2020, pp. 235–248. https://doi.org/10.1007/s40808-019-00674-z.

[13] Halmy M.W.A., Gessler P.E., Hicke J.A., Salem B.B.: *Land use/land cover change detection and prediction in the north-western coastal desert of Egypt using Markov-CA*. Applied Geography, vol. 63, 2015, pp. 101–112. https://doi.org/10.1016/j.apgeog.2015.06.015.

[14] Satya B.A., Shashi M., Deva P.: *Future land use land cover scenario simulation using open source GIS for the city of Warangal, Telangana, India*. Applied Geomatics, vol. 12(3), 2020, pp. 281–290. https://doi.org/10.1007/s12518-020-00298-4.

[15] Yuan F.: *Urban growth monitoring and projection using remote sensing and geographic information systems: A case study in the Twin Cities Metropolitan Area, Minnesota*. Geocarto International, vol. 24(6), 2009, pp. 37–41. https://doi.org/10.1080/10106040903108445.

[16] Maithani S.: *A neural network based urban growth model of an Indian city*. Journal of the Indian Society of Remote Sensing, vol. 37(3), 2009, pp. 363–376. https://doi.org/10.1007/s12524-009-0041-7.

[17] Mohammady S., Delavar M.R., Pahlavani P.: *Urban growth modeling using an artificial neural network: A case study of Sanandaj City, Iran*. The International Archives of the Photogrammetry, Remote Sensing and Spatial Information Sciences, vol. XL-2/W3, 2014, pp. 15–17. https://doi.org/10.5194/isprsarchives-XL-2-W3-203-2014.

[18] Thapa R.B., Murayama Y.: *Scenario based urban growth allocation in Kathmandu Valley, Nepal*. Landscape and Urban Planning, vol. 105(1–2), 2012, pp. 140–148. https://doi.org/10.1016/j.landurbplan.2011.12.007.

[19] Batty M., Longley P.A.: *The fractal simulation of urban structure*. Environment and Planning A: Economy and Space, vol. 18(9), 1986, pp. 1143–1179. https://doi.org/10.1068/a181143.

[20] Tannier C., Pumain D.: *Fractals in urban geography: A theoretical outline and an empirical example*. Cybergeo: European Journal of Geography, 2005, 307. https://doi.org/10.4000/cybergeo.3275.

[21] Kantakumar L.N., Kumar S., Schneider K.: *SUSM: A scenario-based urban growth simulation model using remote sensing data.* European Journal of Remote Sensing, vol. 52(sup. 2), 2019, pp. 26–41. https://doi.org/10.1080/22797254.2019.1585209.

[22] Makse H.A., Havlin S., Stanley H.E.: *Modelling urban growth patterns*. Nature, vol. 377, 1995, pp. 608–612. https://doi.org/10.1038/377608a0.

[23] Motieyan H., Mesgari M.S.: *An agent-based modeling approach for sustainable urban planning from land use and public transit perspectives*. Cities, vol. 81, 2018, pp. 91–100. https://doi.org/10.1016/j.cities.2018.03.018.

[24] Tian G., Qiao Z.: *Modeling urban expansion policy scenarios using an agent-based approach for Guangzhou Metropolitan Region of China*. Ecology and Society, vol. 19(3), 2014, 52. https://doi.org/10.5751/ES-06909-190352.

[25] Samardžić-Petrović M., Dragićević S., Bajat B., Kovačević M.: *Exploring the decision tree method for modelling urban land use change*. Geomatica, vol. 69(3), 2015, pp. 313–325. https://doi.org/10.5623/cig2015-305.

[26] Ishtiaque A., Shrestha M., Chhetri N.: *Rapid urban growth in the Kathmandu Valley, Nepal: Monitoring land use land cover dynamics of a Himalayan city with Landsat imageries*. Environments, vol. 4(4), 2017, 72. https://doi.org/10.3390/environments4040072.

[27] Thapa R.B., Murayama Y.: *Examining spatiotemporal urbanization patterns in Kathmandu Valley, Nepal: Remote sensing and spatial metrics approaches*. Remote Sensing, vol. 1(3), 2009, pp. 534–556. https://doi.org/10.3390/rs1030534.

[28] Karna B.K., Mandal U.K., Bhardwaj A.: *Urban sprawl modeling using RS and GIS technique in Kirtipur Municipality*. Journal on Geoinformatics, Nepal, vol. 12, 2013, pp. 50–56. https://doi.org/10.3126/njg.v12i0.9073.

[29] Regmi R.R., Saha S.K., Subedi D.S.: *Geospatial analysis of land use land cover change modeling in Phewa Lake Watershed of Nepal by using GEOMOD model*. Himalayan Physics, vol. 6–7, 2017, pp. 65–72. https://doi.org/10.3126/hj.v6i0.18363.

[30] Rimal B., Zhang L., Keshtkar H., Haack B.N., Rijal S., Zhang P.: *Land use/land cover dynamics and modeling of urban land expansion by the integration of cellular automata and Markov chain*. ISPRS International Journal of Geo-Information, vol. 7(4), 2018. https://doi.org/10.3390/ijgi7040154.

[31] Government of Nepal, Ministry of Urban Development (MoUD): *National Urban Development Strategy. Part B: Detailed Document*. Kathmandu 2017. https://giwmscdntwo.gov.np/media/pdf_upload/nuds-part-b_1gqrcek.pdf [access: August 19, 2019].

[32] Budha P.B., Bhardwaj A., Thapa R.B.: *Illustration of rapid urban growth in Surkhet Valley of Nepal via land use and land cover dynamics*. Geoplanning: Journal of Geomatics and Planning, vol. 10(2), 2023, pp. 167–178. https://doi.org/10.14710/geoplanning.10.2.167-178.

[33] Rijal S., Rimal B., Sloan S.: *Flood hazard mapping of a rapidly urbanizing city in the foothills (Birendranagar, Surkhet) of Nepal*. Land, vol. 7(2), 2018, 60. https://doi.org/10.3390/land7020060.

[34] Shrestha S.: *Spatio-temporal analysis and modeling of urban growth of Biratnagar City, Nepal*. ISPRS Annals of the Photogrammetry, Remote Sensing and Spatial Information Sciences, vol. IV-5/W2, 2019, pp. 10–11. https://doi.org/10.5194/isprs-annals-IV-5-W2-97-2019.

[35] Pontius R.G., Malanson J.: *Comparison of the structure and accuracy of two land change models*. International Journal of Geographical Information Science, vol. 19(2), 2005, pp. 243–265. https://doi.org/10.1080/13658810410001713434.

[36] Pontius R.G., Huffaker D., Denman K.: *Useful techniques of validation for spatially explicit land-change models.* Ecological Modelling, vol. 179(4), 2004, pp. 445–461. https://doi.org/10.1016/j.ecolmodel.2004.05.010.